3d-printed force sensitive structure using embedded long-period fiber grating

Felipe Oliveira Barino, Renato Luiz Faraco-Filho, Deivid Campos, and Alexandre Bessa dos Santos

*Felipe Oliveira Barino is with the Federal University of Juiz de Fora, 36036-900, Brazil (e-mail: felipe.barino@engenharia.ufjf.br).
Renato Luiz Faraco-Filho is with Federal University of Juiz de Fora, 36036-900, Brazil.
Deivid Campos is with the Federal University of Juiz de Fora, 36036-900, Brazil.
Alexandre Bessa dos Santos is with the Federal University of Juiz de Fora, 36036-900, Brazil
** Corresponding author*

***Abstract*—In this work, we present a low-cost tactile sensor based on arc-induced long-period fiber grating (LPG) embedded in polylactic acid (PLA) by fused deposition modeling (FDM). The 3d printing process used to embed the LPG, offers easy customization, flexibility, fast prototyping, and low-cost fabrication. At the same time, optical fiber sensors such as fiber Bragg gratings (FBGs) and LPGs are compact, resistant, and immune to electromagnetic interference. Therefore, the easy fabrication and low cost of arc-induced LPGs coupled to the 3d printing advantages offer low-cost custom force sensing elements with all the advantages of optical fiber sensors. This way, the proposed tactile sensor is a lightweight, small-size, and cost-effective tactile sensing scheme that offers easy implementation and tailoring to specific applications. In this study, we fabricated, embedded, calibrated, and evaluated the proposed LPG sensor tactile sensor. We showed this approach provided high force sensitivity (11.723 nm.N^{-1}) with high linearity (99.28 %), sub-decimal measurement error, and no drift.**

Keywords—optical sensor, force sensing, fused deposition modeling, tactile sensor

I. Introduction

Tactile sensors are used to measure forces applied to a structure and are extremely important in several fields, from structural engineering to medicine. And recently these sensors have become more important due to the rise of robotics, since it is essential for the perception and control of robots. In fact, force sensing is a subject that has gained attention since the beginning of robotics [1]. The tactile sensor can lead to shape mapping through touch, which is necessary both for dexterous manipulation and safe human-robot interaction [2].

Optical fiber sensors are good candidates for tactile sensing due to its strain sensitivity; this field of optics has been gaining attention due to the sensor's compact size, high corrosion resistance, good stability, electromagnetic noise immunity, ease of multiplexing, and data transport. Based on these intrinsic characteristics of optical fiber sensors, they have been employed in several industries. The lack of electrical current improves the safety of measurements where the risks of fire or explosions are a concern, in [3] the authors report on a fiber Bragg grating (FBG) sensor to measure flow rate in the oil and gas industry, for example. The electromagnetic noise immunity also benefitted the use of fiber-based sensors to monitor in-service overhead transmission conductors [4].

As for the tactile and force-related sensors, a touch-sensitive surface made of Polydimethylsiloxane embedded with several FBG strain sensors was presented in [5]; moreover, in [6] the authors presented an FBG also embedded in a polymer for tactile

sensing. The work reported in [7], on the other hand, used FBG embedded in silicon, and authors of [8] presented a setup for contact force and stress measurement in articular joints using FBGs as well.

3d printing is a manufacturing process known to be an important technology of the third industrial revolution [9], the process is capable of fast prototyping, offers on-demand fabrication of complex structures with efficient use of materials. Recently this technology has been used to embed complex structures and devices into various types of designs [10–14], including FBG strain sensors for structural health monitoring [15], FBG based pressure sensor [13], and 3d-printed wearables with optical fiber-based temperature, humidity, and force sensing [14]. At the same time, projects involving robotics and prosthetics are widely employing 3d printing technology [16–21] due to its ease prototyping and manufacturing.

In this context, we present a simple and low-cost optical fiber-based tactile sensor embedded in polylactic acid (PLA) by fused deposition modeling (FDM), which is one of the most used and accessible kinds of 3d printing techniques. The intrinsic characteristics of optical fiber sensors make them good candidates for several force sensing applications and the 3d printing embedment of such sensors could favor the structural monitoring and touch-responsiveness of 3d printed structures, thus expanding the serviceability and usefulness of 3d printed parts and devices.

The optical sensor used for this task is a long-period fiber grating (LPG), an easy to manufacture and low-cost fiber grating sensor. Fiber gratings are optical devices built into the optical fiber by periodically modifying its properties [22]. FBGs are also fiber grating devices and, although their use is widely reported as strain sensors in robotics [5–7], they could be difficult and expensive to manufacture. The sub-micron period of FBGs requires expensive manufacturing processes and equipment, while LPGs can be manufactured using simply a fusion spicing machine [23].

Beyond the ease of manufacturing, the transmission spectrum of LPGs is more complex, thus incorporating more information; for this reason, a single LPG can be used in multi-parameter or multi-dimensional sensing [24–27], whereas similar FBG-based approaches generally require a higher transducer count [28–30].

The packaging of optical fiber grating sensors using a 3d printer was introduced recently in [31,32], but the authors only introduced the technology for FBG sensors and they proposed the 3d printing encapsulation mostly to allow better adhesion of the FBG to the sensing structure. Therefore, the manufacturing of 3d-printed smart structures using optical fiber grating strain sensors embedded into the structure itself has not been fully investigated. In this work, we propose the embedment of LPGs into a 3d-printed structure to measure the force applied to this structure. To the best of our knowledge, the embedment of an LPG sensor into a 3d-printed structure to make this structure sensitive to external forces was never investigated. A scheme of our proposal is shown in Fig. 1, where one can see the 3d-printed structure with the optical fiber and the fiber grating device (LPG) embedded in it (Fig. 1a), and the effect of an external force acting on the touch-sensitive structure (Fig. 1b).

II. Methods

LPGs are manufactured by periodically changing the optical fiber properties, such as refractive index and geometry; this period varies from dozens to hundreds of micrometers [22]. This periodic structure couples the guided mode from the fiber core to evanescent cladding modes, and since scattering occurs at the interface between

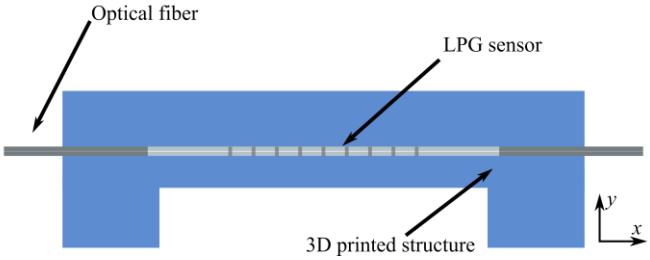

(a) Proposed tactile sensor scheme.

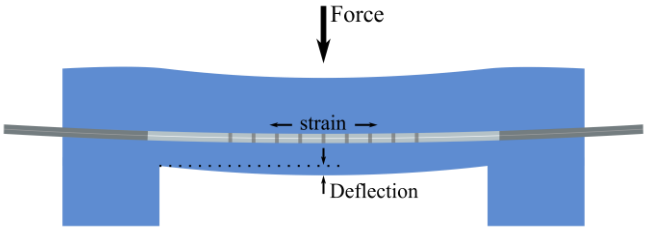

(b) Application of an external force.

Fig. 1. Scheme of the proposed touch-sensitive 3d-printed structure, (a) shows the optical fiber embedded into the 3d-printed material and (b) the LPG strained by application of a force into the 3d-printed structure.

cladding and external media, optical power is lost at the wavelength in which light is coupled. This wavelength is named resonant wavelength (λ_{res}) and is given by [22,33]:

$$\lambda_{res}^{m} = \left(n_{eff,co} - n_{eff,cl}^{m}\right) \cdot \Lambda \tag{1}$$

where λ_{res}^{m} is the m^{th} resonant wavelength, Λ is the grating period, $n_{eff,co}$ is the core mode effective index, whereas $n_{eff,cl}^{m}$ is the m^{th} cladding mode effective index. These last two parameters changes when the device is stressed by 1) physical deformation, causing a change in the grating period; and 2) changes in the refractive index due to the photo-elastic effect. Hence, the strain sensitivity of LPGs is given by:

$$\frac{\partial \lambda_{res}}{\partial \epsilon} = \lambda_{res} \cdot \gamma \cdot (1 + \Gamma_{strain}) \tag{2}$$

$$\Gamma_{strain} = \frac{\eta_{co} n_{eff,co} - \eta_{cl} n_{eff,cl}^{m}}{n_{eff,co} - n_{eff,cl}^{m}} \tag{3}$$

where the subscript co denotes the core and cl cladding properties and η is the elasto-optic coefficient. Therefore, we can correlate an external force applied to the 3d-printed structure (as illustrated in Fig. 1b) to a resonant wavelength shift and use the device as a tactile sensor by measuring the LPG resonant wavelength.

Let F be the intensity of a force illustrated in Fig. 1b, applied to the central point of the upper face of the tactile-sensitive 3d-printed structure. For simplification, consider this structure a simply supported beam with length L between the support reactions, then, the bending moment $M(x)$ is given by:

$$\frac{\mathrm{d}M(x)}{\mathrm{d}x} = V(x) \tag{4}$$

$$\frac{\mathrm{d}V(x)}{\mathrm{d}x} = w(x) = F \cdot \delta\left(x - \frac{L}{2}\right) \tag{5}$$

where $V(x)$ is the shear force, $w(x)$ is the loading function, and $\delta(x)$ is the delta function used to represent a point force.

Using the calculated bending moment at a given point, the strain is calculated by:

$$\epsilon = -\frac{M(x)y\prime}{E\,I} \tag{6}$$

where E is the material Young modulus, I the beam's moment of inertia, and y' the distance between the point and the neutral plane along the y-axis.

Therefore, by measuring the point-strain using the embedded LPG sensor, one can infer the intensity of the force applied to the 3d-printed structure. Note that two variables of eq. (6) are free to be changed during the sensor manufacturing, the sensor position y' and the beam's moment of inertia I. Moreover, the strain measured by the LPG sensor would be affected by these variables even if the loading condition remains the same. Therefore, the force sensitivity could be increased by reducing the structure's moment of inertia or by placing the LPG further away from the neutral plane. The force measurement range could also be tailored by changing the structure stiffness; this could be accomplished by changing the material or simply the beam thickness. But note that changing the thickness presents a tradeoff between measurement range and sensitivity because the thickness would affect the moment of inertia and, consequently the force sensitivity. Moreover, these parameters can be easily changed due to the 3d printing low design-to-manufacture time.

Note that two points that share the same x coordinate and the same distance from the neutral plane but at opposite sides would have the same strain intensity, with opposite sign. Therefore, the proposed approach force sensor could be easily modified to perform temperature-insensitive measurements using a differential approach similar to what was demonstrated in [34]. Additionally, encapsulation should also reduce the refractive index cross-sensitivity of the final sensor by itself.

The LPG used in this work was manufactured using the arc-electric technique [23], a point-by-point method of inducing refractive index and radius modulation in optical fibers. The sensor was fabricated in standard single-mode optical communication fiber, SMF-28, with a period of 500.0 ± 0.5 µm and 20 segments. Then we designed a parallelepiped with 100 mm x 10 mm x 1 mm dimensions and 3d-printed in PLA using a MakerBot Replicator Z18 3d printer.

The LPG was embedded in this structure by stopping the printing process at the desired thickness (variable y' of eq. (6)), placing the sensor centered on the structure surface, parallel to the x-axis, and without pre-tensioning the optical fiber; after the sensor was correctly positioned, the printing process was resumed, as previously

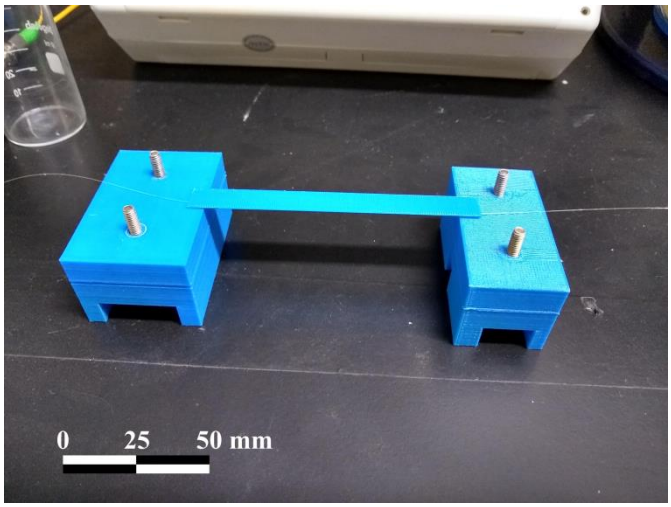

Fig. 2. Photography of the tactile sensor, with the optical fiber containing the LPG embedded into the 3d-printed structure.

reported for FBG strain sensors [31,32]. The resulting touch-sensitive 3d-printed structure, i.e. tactile sensor, ready for calibration can be seen in Fig 2.

To calibrate the sensor, we placed four different weights on top of the 3d-printed structure shown in Fig. 2, to emulate the force illustrated in Fig. 1b. The process of loading the sensor was repeated four times for each one of the five loads: 0 g (free load), 52.0±0.5 g, 83.0±0.5 g, 103.0±0.5 g, and 114.0±0.5 g. The load was placed on top of the structure, centering the mass at the structure's upper surface center; therefore, the mass centerline matches the central point of the upper face. Throughout the process we measured and recorded the LPG spectrum using an Optical Spectrum Analyzer (OSA), in a temperature-controlled environment (20°C), to determine the LPG resonant wavelength in each loading scenario. Therefore the optical setup used was: an OptoLink ELED light source centered near 1550 nm, the designed tactile sensor, and a ThorLabs OSA203 OSA.

After collecting the spectral data, we fitted the LPG transmission spectra to a Gaussian around the resonance dip to determine the resonant wavelength [35]. After that, we obtained the calibration curve and analyzed the sensing scheme by the obtained R^2, root mean squared error (RMSE), and we also estimated the bias and standard deviation of the sensing scheme by statistical analysis of the fitted model residues. Furthermore, we tested the sensor stability with an 83 g weight and free load for 15 min. and analyzed the measurements.

III. Results

The results obtained in the sensor characterization are presented in Fig. 3 and Fig. 4, the first shows the embedded LPG spectral response under the five different loads used in sensor calibration, the latter shows the calibration curve obtained by the extracted resonant wavelength from spectra.

From the measured spectra, one can see that when the load increases and therefore, the applied force also increases, the spectrum dip shifts to higher wavelengths. Hence, the resonant wavelength of the embedded LPG increases proportionally with the force applied to the sensing structure. From the calibration curve shown in Fig. 4, we could see that the relationship between applied load and LPG's resonant wavelength is linear.

Therefore we adjusted the experimental data to a linear function and obtained that the LPG sensitivity to the applied load was 0.115±0.011 nm.g^{-1}, while the calibration curve linear coefficient was 1455.6±0.9 nm. Therefore, the sensor's force sensitivity was

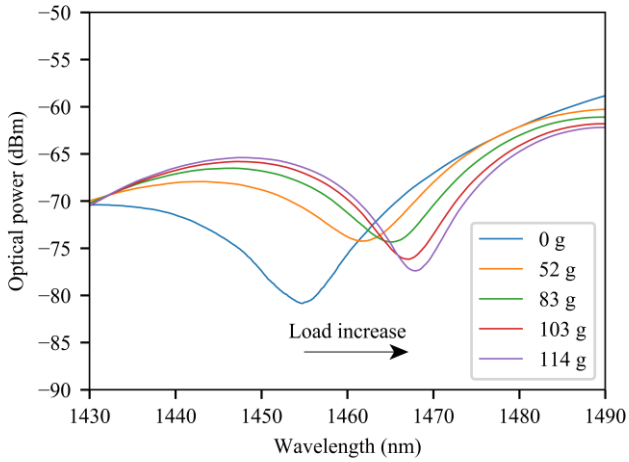

Fig. 3. LPG embedded in PLA spectrum for different loads (forces).

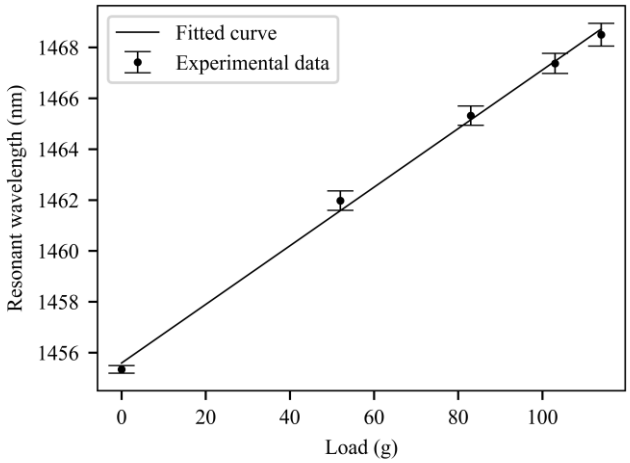

Fig. 4. Tactile sensor calibration curve.

11.723 nm.N^{-1}, considering the gravitational acceleration as 9.81 m.s^{-2}. This linear model fitted to represent the sensor response to external loads explained well the experimental results, with R^2 of 0.9973 and an RMSE of 3.44 g.

Additionally, we present the curve fitting residues in Fig. 5, on the left y-axis side the histogram frequency for the residues is shown, while the right y-axis presents the estimated residual probability density function (pdf). We could see by the histogram that the residues tended to a Gaussian pdf, which we estimated by the parametric fitting of the residues. The estimated Gaussian pdf mean and standard deviation were, respectively, μ=0.00 g and σ=3.44 g. These Gaussian parameters are, within the 95% confidence intervals, μ=0$\pm$1.65 g and $\sigma \in$ (2.68, 5.16) g. Moreover, the χ^2 and Kolmogorov-Smirnov tests did not reject the hypotheses that the distribution of the residuals is indeed the fitted pdf.

Table I summarizes the principal characteristics of the proposed tactile sensor, obtained during the calibration and characterization procedures, in terms of the applied load itself and converting it to force. Note that the proposed tactile sensing technique was quite sensitive and, by analyzing the residues we concluded that the applied force could be estimated by the sensor with 0.06 N uncertainty, considering a 95% confidence interval. Note that this uncertainty was estimated by fitting the calibration residues to a normal distribution, due to the small number of data points used to calibrate the sensor, this estimation tends to overestimate the uncertainty. Later we tested the sensor with

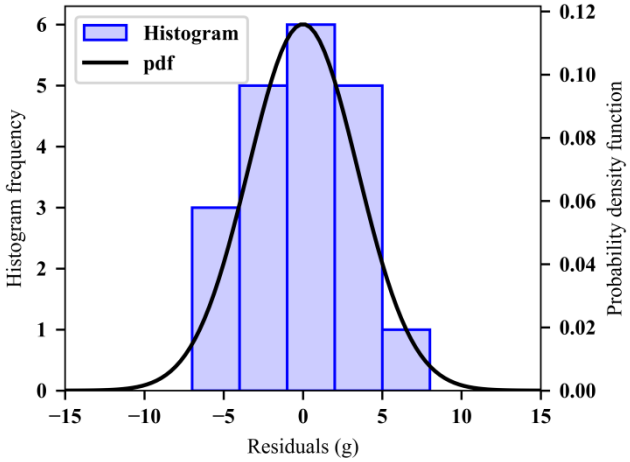

Fig. 5. Tactile sensor calibration curve residues.

Table I
Characteristics of the lpg tactile sensor embedded in 3d printing structure.

		Load	Force
	Sensitivity	115 pm.g^{-1}	11.723 nm.N^{-1}
	R^2	0.9973	
Calibration residues	μ	0.00 g	0.000 N
	σ	3.44 g	0.033 N

known mass to evaluate the sensor under a practical and more realistic measurement procedure.

The results of these static measurements for free load and 83 g are shown in Fig. 6; note that the applied force was 0.81423 N for the 83 g mass. These measurements were collected over 15 min. with a sampling interval of 3 s, for each loading condition. Therefore, Fig. 6 shows two individual experiments and the x-axis represents the data collection time for each loading experiment. One can see that the proposed sensor didn't drift, showing good stability. Furthermore, the Gaussian pdf obtained from the collected data, by parametric estimation, is shown on the right-hand side of the graph. A standard deviation of 0.0081 N and 0.0046 N was calculated for free load and 0.81423 N, respectively. Observe that the uncertainty estimated by the calibration curve was indeed super estimated, the static tests showed a maximum uncertainty of 0.016 N, considering a 95% confidence interval, which falls within the previously estimated uncertainty interval, and shows that under practical use the sensor presents low uncertainty.

Previous FBG-based transverse load/tactile sensors reported in the literature showed force sensitivity at least one order of magnitude smaller than the obtained in this work. The authors of [30] used several FBGs sensors to manufacture a fingertip tactile sensor obtaining a sensitivity of 71 pm/N at the x-axis and their practical force measurements showed resolutions of only about 0.15 N. Whereas the touch-sensitive 3x3 FBG array presented in [36] showed a 0.005 N resolution using a rather complex and nonlinear setup with 1 nm.N^{-1} sensitivity. The high sensitivity force sensor presented in [37], on the other hand, showed a sensitivity of 2.5 nm.N^{-1} in bare fiber when considering the peak-to-peak distance after the splitting of the reflection FBG spectrum due to the birefringence introduced by the transverse force, but their approach showed high nonlinearity and little effect under lower forces (<80 N). Therefore, our results showed the proposed tactile sensing scheme using the LPG embedded into a 3d-printed

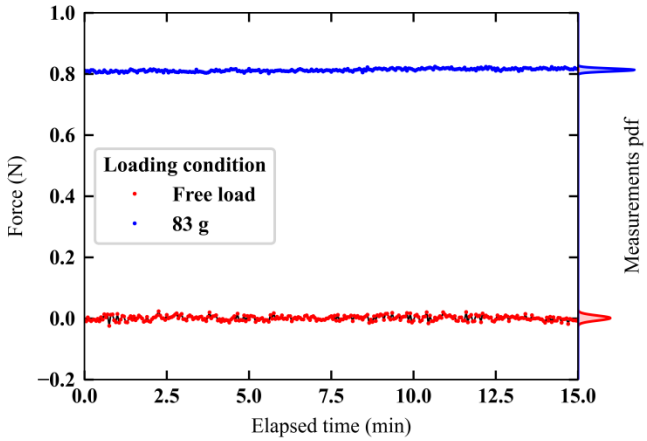

Fig. 6. Static measurements.

improved the optical fiber tactile sensor sensitivity to external forces, comparing to these works found in the literature, especially for forces as small as the weight of a 5 g mass.

IV. Conclusion

In this study, we presented the design and fabrication of an optical fiber-based tactile sensor. Our approach consisted of embedding an LPG in a 3d-printed structure by placing the LPG sensor into the structure during its fabrication. The LPG ease of manufacture alongside the rapid prototyping of 3d printing is the main advantage of our proposal.

Our experiments showed the designed LPG tactile sensor embedded in a 3d-printed structure had a sensitivity of 11.723 $nm.N^{-1}$ and R^2=0.9973. Static tests with known forces showed maximum uncertainty of 0.016 N and great stability. Moreover, the ease of fabrication can be used to explore different designs and to manufacture various touch-sensitive structures that could be tailored to specific applications. Further investigation concerning temperature and refractive index cross-sensitivity of the proposed sensor is highly valuable for several applications and should be incorporated in the future.

Acknowledgments

This work was supported in part by the Programa de Bolsas de Pós-graduação (PBPG-UFJF) through the Programa de Pós-graduação em Engenharia Elétrica (PPEE-UFJF), Coordenação de Aperfeiçoamento Pessoal de Nível Superior (CAPES), Conselho Nacional de Desenvolvimento Científico e Tecnológico (CNPq), Instituto Nacional de Energia Elétrica (Inerge-UFJF), and Transmissoras Brasileiras de Energia (TBE).

References

[1] Y.-J. Ge, J.-J. Zhang, Y. Ge, Z.-C. Wu, L.-F. Gao, Ubiquitous sensing and robot perception, Acta Autom. Sin. 28 (2002) 125–133.

[2] B. Navarro, A. Fonte, P. Fraisse, G. Poisson, A. Cherubini, In pursuit of safety: An open-source library for physical human-robot interaction, IEEE Robot. Autom. Mag. 25 (2018) 39–50.

[3] A.S. Allil, F. da S. Dutra, A. Dante, C.C. Carvalho, R.C. da S.B. Allil, M.M. Werneck, FBG-Based Sensor Applied to Flow Rate Measurements, IEEE Trans. Instrum. Meas. 70 (2021) 1–8. https://doi.org/10.1109/TIM.2020.3014751.

[4] D.H. Waters, J. Hoffman, M. Kumosa, Monitoring of Overhead Transmission Conductors Subjected to Static and Impact Loads Using Fiber Bragg Grating Sensors, IEEE Trans. Instrum. Meas. 68 (2019) 595–605. https://doi.org/10.1109/TIM.2018.2851698.

[5] G.T. Kanellos, G. Papaioannou, D. Tsiokos, C. Mitrogiannis, G. Nianios, N. Pleros, Two dimensional polymer-embedded quasi-distributed FBG pressure sensor for biomedical applications, Opt. Express. 18 (2010) 179–186.

[6] C. Yan, E. Ferraris, T. Geernaert, F. Berghmans, D. Reynaerts, Development of flexible pressure sensing polymer foils based on embedded fibre Bragg grating sensors, Procedia Eng. 5 (2010) 272–275.

[7] J. Song, Q. Jiang, Y. Huang, Y. Li, Y. Jia, X. Rong, R. Song, H. Liu, Research on

pressure tactile sensing technology based on fiber Bragg grating array, Photonic Sensors. 5 (2015) 263–272.

[8] C.R. Dennison, P.M. Wild, D.R. Wilson, M.K. Gilbart, An in-fiber Bragg grating sensor for contact force and stress measurements in articular joints, Meas. Sci. Technol. 21 (2010) 115803. https://doi.org/10.1088/0957-0233/21/11/115803.

[9] B. Berman, 3-D printing: The new industrial revolution, Bus. Horiz. 55 (2012) 155–162.

[10] B.Y. Ahn, E.B. Duoss, M.J. Motala, X. Guo, S.-I. Park, Y. Xiong, J. Yoon, R.G. Nuzzo, J.A. Rogers, J.A. Lewis, Omnidirectional printing of flexible, stretchable, and spanning silver microelectrodes, Science (80-.). 323 (2009) 1590–1593.

[11] L.E. Bertassoni, M. Cecconi, V. Manoharan, M. Nikkhah, J. Hjortnaes, A.L. Cristino, G. Barabaschi, D. Demarchi, M.R. Dokmeci, Y. Yang, others, Hydrogel bioprinted microchannel networks for vascularization of tissue engineering constructs, Lab Chip. 14 (2014) 2202–2211.

[12] J.T. Muth, D.M. Vogt, R.L. Truby, Y. Mengüç, D.B. Kolesky, R.J. Wood, J.A. Lewis, Embedded 3D printing of strain sensors within highly stretchable elastomers, Adv. Mater. 26 (2014) 6307–6312.

[13] C. Hong, Y. Zhang, L. Borana, Design, fabrication and testing of a 3D printed FBG pressure sensor, IEEE Access. 7 (2019) 38577–38583.

[14] A.G. Leal-Junior, C.R. D\'\iaz, M.J. Pontes, C. Marques, A. Frizera, Polymer optical fiber-embedded, 3D-printed instrumented support for microclimate and human-robot interaction forces assessment, Opt. Laser Technol. 112 (2019) 323–331.

[15] L. Fang, T. Chen, R. Li, S. Liu, Application of embedded fiber Bragg grating (FBG) sensors in monitoring health to 3D printing structures, IEEE Sens. J. 16 (2016) 6604–6610.

[16] A. Stroud, M. Morris, K. Carey, J.C. Williams, C. Randolph, A.B. Williams, MU-L8: The design architecture and 3D printing of a Teen-Sized humanoid soccer robot, in: 8th Work. Humanoid Soccer Robot. IEEE-RAS Int. Conf. Humanoid Robot. Atlanta, GA, 2013.

[17] M. Lapeyre, P. Rouanet, J. Grizou, S. N'Guyen, A. Le Falher, F. Depraetre, P.-Y. Oudeyer, Poppy: Open source 3D printed robot for experiments in developmental robotics, in: 4th Int. Conf. Dev. Learn. Epigenetic Robot., 2014: pp. 173–174.

[18] S. Ziaeefard, G.A. Ribeiro, N. Mahmoudian, GUPPIE, underwater 3D printed robot a game changer in control design education, in: 2015 Am. Control Conf., 2015: pp. 2789–2794.

[19] Y. Tlegenov, K. Telegenov, A. Shintemirov, An open-source 3D printed underactuated robotic gripper, in: 2014 IEEE/ASME 10th Int. Conf. Mechatron. Embed. Syst. Appl., 2014: pp. 1–6.

[20] J. Zuniga, D. Katsavelis, J. Peck, J. Stollberg, M. Petrykowski, A. Carson, C. Fernandez, Cyborg beast: a low-cost 3d-printed prosthetic hand for children with upper-limb differences, BMC Res. Notes. 8 (2015) 1–9.

[21] K.F. Gretsch, H.D. Lather, K. V Peddada, C.R. Deeken, L.B. Wall, C.A. Goldfarb, Development of novel 3D-printed robotic prosthetic for transradial amputees, Prosthet. Orthot. Int. 40 (2016) 400–403.

[22] T. Erdogan, Fiber grating spectra, J. Light. Technol. 15 (1997) 1277–1294.

[23] G. Rego, Arc-induced long period fiber gratings, J. Sensors. 2016 (2016).

[24] F. Barino, F.S. Delgado, M.A. Jucá, T.V.N. Coelho, A. Bessa dos Santos, Comparison of regression methods for transverse load sensor based on optical fiber long-period grating, Measurement. 146 (2019) 728–735. https://doi.org/10.1016/j.measurement.2019.07.017.

[25] Y. Huang, B. Chen, G. Chen, H. Xiao, S.U. Khan, Simultaneous detection of liquid level and refractive index with a long-period fiber grating based sensor device, Meas. Sci. Technol. 24 (2013) 095303. https://doi.org/10.1088/0957-0233/24/9/095303.

[26] J. Zhang, Y. Zhang, L. Zhang, W. Zhang, L. Wang, T. Yan, Two-axis bending vector sensor based on a long-period fiber grating cascading with a hump-shaped taper, Meas. Sci. Technol. 29 (2018) 095107. https://doi.org/10.1088/1361-6501/aad4d5.

[27] Y. Huang, Z. Zhou, Y. Zhang, G. Chen, H. Xiao, A Temperature Self-Compensated LPFG Sensor for Large Strain Measurements at High Temperature, IEEE Trans. Instrum. Meas. 59 (2010) 2997–3004. https://doi.org/10.1109/TIM.2010.2047065.

[28] A.F. Fernandez, F. Berghmans, B. Brichard, P. Mégret, M. Decréton, M. Blondel, A. Delchambre, Multi-component force sensor based on multiplexed fibre Bragg grating strain sensors, Meas. Sci. Technol. 12 (2001) 810–813. https://doi.org/10.1088/0957-0233/12/7/310.

[29] S. He, X. Dong, K. Ni, Y. Jin, C.C. Chan, P. Shum, Temperature-insensitive 2D tilt sensor with three fiber Bragg gratings, Meas. Sci. Technol. 21 (2010) 025203. https://doi.org/10.1088/0957-0233/21/2/025203.

[30] Y.-L. Park, S.C. Ryu, R.J. Black, K.K. Chau, B. Moslehi, M.R. Cutkosky, Exoskeletal force-sensing end-effectors with embedded optical fiber-Bragg-grating sensors, IEEE Trans. Robot. 25 (2009) 1319–1331.

[31] W. Yan, S. Ma, H. Wang, X. Zhang, Fiber Bragg grating online packaging technology based on 3D printing, Opt. Laser Technol. 131 (2020) 106443. https://doi.org/10.1016/j.optlastec.2020.106443.

[32] P. Di Palma, A. Iadicicco, S. Campopiano, Study of fiber Bragg gratings embedded in 3D-printed patches for deformation monitoring, IEEE Sens. J. (2020) 1–1. https://doi.org/10.1109/JSEN.2020.3004280.

[33] Xuewen Shu, Lin Zhang, I. Bennion, Sensitivity characteristics of long-period fiber gratings, J. Light. Technol. 20 (2002) 255–266.

[34] C. Hong, Y. Zhang, Z. Lu, Z. Yin, A FBG Tilt Sensor Fabricated Using 3D Printing Technique for Monitoring Ground Movement, IEEE Sens. J. 19 (2019) 6392–6399. https://doi.org/10.1109/JSEN.2019.2908873.

[35] G.R.C. Possetti, R.C. Kamikawachi, M. Muller, J.L. Fabris, Metrological Evaluation of Optical Fiber Grating-Based Sensors: An Approach Towards the Standardization, J. Light. Technol. 30 (2012) 1042–1052. https://doi.org/10.1109/JLT.2011.2167500.

[36] J.-S. Heo, J.-H. Chung, J.-J. Lee, Tactile sensor arrays using fiber Bragg grating sensors, Sensors Actuators A Phys. 126 (2006) 312–327. https://doi.org/10.1016/j.sna.2005.10.048.

[37] Y. Wang, M. Wang, X. Huang, High-sensitivity fiber Bragg grating transverse force sensor based on centroid measurement of polarization-dependent loss, Meas. Sci.

Technol. 21 (2010) 065304. https://doi.org/10.1088/0957-0233/21/6/065304.